Available online at www.sciencedirect.com
ScienceDirect
Biochimica et Biophysica Acta 1778 (2008) 1067–1078
Biochimica et Biophysica Acta BBA
www.elsevier.com/locate/bbamem

Effect of hydrostatic pressure on the bilayer phase behavior of symmetric and asymmetric phospholipids with the same total chain length

Masaki Goto [b], Masataka Kusube [c], Nobutake Tamai [a,b], Hitoshi Matsuki [a,b,*], Shoji Kaneshina [a,b]

[a] *Department of Life System, Institute of Technology and Science, The University of Tokushima, 2-1 Minamijosanjima-cho, Tokushima 770-8506, Japan*
[b] *Department of Biological Science and Technology, Faculty of Engineering, The University of Tokushima, 2-1 Minamijosanjima-cho, Tokushima 770-8506, Japan*
[c] *Department of Materials Science and Engineering, Wakayama National College of Technology, 77 Nada, Noshima, Gobo, Wakayama 644-0023, Japan*

Received 18 September 2007; received in revised form 10 December 2007; accepted 12 December 2007
Available online 23 December 2007

Abstract

The bilayer phase transitions of palmitoylstearoyl-phosphatidylcholine (PSPC), diheptadecanoyl-PC (C17PC) and stearoylpalmitoyl-PC (SPPC) which have the same total carbon numbers in the two acyl chains were observed by differential scanning calorimetry and high-pressure optical method. As the temperature increased, these bilayers exhibited four phases of the subgel (L_c), lamellar gel (L_β'), ripple gel (P_β') and liquid crystal (L_α), in turn. The L_c phase was observed only in the first heating scan after cold storage. The temperatures of the phase transitions were almost linearly elevated by applying pressure. The temperature–pressure phase diagrams and the thermodynamic quantities associated with the phase transitions were compared among the lipid bilayers. For all the bilayers studied, the pressure-induced interdigitated gel ($L_\beta I$) phase appeared above the critical interdigitation pressure (CIP) between the L_β' and P_β' phases. The CIPs for the PSPC, C17PC and SPPC bilayers were found to be 50.6, 79.1 and 93.0 MPa, respectively. Contribution of two acyl chains to thermodynamic properties for the phase transitions of asymmetric PSPC and SPPC bilayers was not even. The *sn*-2 acyl chain lengths of asymmetric PCs governed primarily the bilayer properties. The fluorescence spectra of Prodan in lipid bilayers showed the emission maxima characteristic of bilayer phases, which were dependent on the location of Prodan in the bilayers. Second derivative of fluorescent spectrum exhibited the original emission spectrum of Prodan to be composed of the distribution of Prodan into multiple locations in the lipid bilayer. The F''_{497}/F''_{430} value, a ratio of second derivative of fluorescence intensity at 497 nm to that at 430 nm, is decisive evidence whether bilayer interdigitation will occur. With respect to the $L_\beta'/L_\beta I$ phase transition in the SPPC bilayer, the emission maximum of Prodan exhibited the narrow-range red-shift from 441 to 449 nm, indicating that the $L_\beta I$ phase in the SPPC bilayer has a less polar "pocket" formed by a space between uneven terminal methyl ends of the *sn*-1 and *sn*-2 chains, in which the Prodan molecule remains stably.

Keywords: Asymmetric phospholipid; Bilayer membrane; Fluorescence; Interdigitation; Phase transition; Pressure

1. Introduction

Application of high pressure as well as temperature to lipid bilayer membranes has provided further understanding of pressure–anesthetic antagonism [1], pressure adaptation in deep sea organisms [2] and high-pressure sterilization in food processing [3–6]. Biological membranes of organisms living in various environments contain many kinds of phospholipids. The phospholipids are amphipathic molecules consisting of polar and non-polar moieties connected by a region of glycerol backbone. With few exceptions, the hydrophobic region consists of two relatively long-chain fatty acids. Earlier studies on the properties of phospholipids in model membranes have concentrated on the symmetric-chain phospholipids which contain two hydrocarbon chains with equal carbon number and degree of unsaturation. Especially, the symmetric phosphatidylcholines (PCs) containing the same acyl chains in the *sn*-1 and *sn*-2 positions on the glycerol backbone such as dipalmitoylphosphatidylcholine (DPPC) have been thoroughly examined by several physico-

* Corresponding author. Department of Life System, Institute of Technology and Science, The University of Tokushima, 2-1 Minamijosanjima-cho, Tokushima 770-8506, Japan. Tel.: +81 88 656 7513; fax: +81 88 655 3162.
E-mail address: matsuki@bio.tokushima-u.ac.jp (H. Matsuki).

0005-2736/$ - see front matter © 2007 Elsevier B.V. All rights reserved.
doi:10.1016/j.bbamem.2007.12.009

chemical techniques in high-pressure studies [7–16]. These measurements have revealed the phase behavior of the DPPC bilayer membrane. Recently we have also constructed the temperature (T)–pressure (p) phase diagrams for homologs of symmetric PC bilayer membranes and revealed that the phase behavior is obviously influenced by the acyl chain length of the PCs [17].

On the other hand, regarding PC molecules in cell membranes, the two chains of the hydrophobic region are usually different, which are called asymmetric PCs. Some investigations on the asymmetric PCs under ambient pressure were also performed by conventional differential scanning calorimetry (DSC) [18–25], high-sensitivity DSC [26–29], X-ray diffraction [23,25,29], Raman and IR spectroscopy [29–33] and NMR [33,34]. A consistent feature on all studies on the asymmetric PC bilayers is that the contribution of two acyl chains to thermodynamic properties associated with bilayer phase transitions was not even [18]. In the case of the two saturated acyl chains, the bilayer of lipids having a longer chain in the *sn*-2 position of glycerol always exhibits significantly higher main-transition temperature (T_m) and enthalpy changes (ΔH) than those for the position-reversed isomer. It is well known for lipids in cell membranes that the *sn*-1 acyl chain is typically saturated, whereas the *sn*-2 acyl chain is usually unsaturated and has different carbon number compared with the *sn*-1 acyl chain [35]. The phenomena can be rationalized on the basis of the known conformational difference between the *sn*-1 and *sn*-2 acyl chains of PCs. The conformational inequivalence of the acyl chains in bilayer membrane of a symmetric PC results in the *sn*-2 acyl chain being 1.5 carbon–carbon bond lengths virtually shorter than the *sn*-1 acyl chain in the gel phase [36]. Therefore, in the case of asymmetric PC bilayers, the difference at terminal methyl ends between the *sn*-1 and *sn*-2 acyl chains changes variously. It is reported that membranes of asymmetric PCs promote the formation of the subgel (so-called lamellar crystal phase) and the interdigitated gel phase when the effective length mismatch between the *sn*-1 and *sn*-2 acyl chains is very great [35,37].

However, there has been no report of the pressure effect on the bilayers of asymmetric PCs containing saturated fatty acids with different chain lengths in the *sn*-1 and *sn*-2 positions. In the present study, the bilayer phase behavior of two kinds of asymmetric PC, 1-palmitoyl-2-stearoyl-PC (PSPC) and 1-stearoyl-2-palmitoyl-PC (SPPC), in which the distance at terminal methyl ends between the *sn*-1 and *sn*-2 chains are 0.5 and 3.5 carbon–carbon lengths, respectively [36], is observed under ambient and high pressures. The thermotropic and barotropic phase behavior of the asymmetric PC bilayer membranes is discussed by comparing the T–p phase diagram, thermodynamic quantities and spectra of fluorescence probe 6-propionyl-2-(dimethylamino) naphthalene (Prodan) in PSPC and SPPC bilayer membranes with those of the symmetric PC series. In particular, the bilayer of symmetric diheptadecanoyl-PC (C17PC) which has the same total carbon numbers in the two acyl chains as PSPC and SPPC is effectively used for direct comparison of the contribution of two acyl chains to thermodynamic properties of bilayer phase transitions.

2. Experimental

2.1. Materials

Asymmetric lipids, 1-palmitoyl-2-stearoyl-*sn*-glycero-3-phosphocholine (Lot# 160-180PC-17) and 1-stearoyl-2-palmitoyl-*sn*-glycero-3-phosphocholine (Lot#180-160PC-16), and a symmetric lipid, 1,2-diheptadecanoyl-*sn*-glycero-3-phosphocholine (Lot#170PC-27), were purchased from Avanti Polar Lipids, Inc. (Alabaster, AL) and used as received. The fluorescence probe, 6-propionyl-2-(dimethylamino)naphthalene, was obtained from Molecular Probes, Inc. (Eugine, OR). Water was distilled twice from a dilute alkaline permanganate solution.

We employed two methods of vesicle preparation. One is the sonication method. The phospholipid multilamellar vesicles were prepared by suspending each phospholipid in water at 1.0 mmol kg^{-1} (0.076 wt %). This method was used for DSC measurement and light-transmittance measurement. The suspensions were sonicated for a few minutes by using a sonifier (Branson Model 3510J-DTH) at a temperature several degrees above the main-transition temperature for each lipid. These dispersions were annealed by repeating thermal cycling at least seven times between freeze storage at −30 °C (for one day) and cold storage at 5 °C (for one day) and subsequently refrigerated to induce the lamellar crystal phase. The other was followed by Bangham's method [38] which was used for fluorescence measurements. The chloroform stock solution of a lipid was mixed with an ethanol solution of Prodan. The mixed solution was dried in vacuum to remove all residual solvents and finally to get a dry film. Water was added to the dry film and the lipid samples were hydrated by a treatment of vortex. The suspensions were sonicated at a temperature above the main-transition temperature for each lipid for a short time (ca. 3 min) in order to prepare the multilamellar vesicle suitable for the fluorescence measurements. The total concentration of the lipid was 1.0 mmol kg^{-1} and the molar ratio of Prodan to the lipid was 1:500. The sample solutions were protected from light until measurements.

2.2. Differential scanning calorimetry

The phase transitions of phospholipid multilamellar vesicles under ambient pressure were observed by a MicroCal MCS high-sensitivity differential scanning calorimeter (Northampton, MA). The heating rate was 0.75 K min^{-1}. The enthalpy changes of phase transitions were determined from the endothermic peak areas as average values over several DSC measurements.

2.3. Light-transmittance measurements under high pressure

The phase transitions of C17PC, PSPC and SPPC bilayer membranes were observed under high pressure by two kinds of optical methods, the isobaric thermotropic and isothermal barotropic techniques, which were described previously [15]. The pressures were monitored within an accuracy of 0.2 MPa by using a Heise gauge. The temperature of high-pressure cell was controlled within ± 0.1 °C by circulating water from a water bath through the jacket enclosing the measurement cell. With respect to isobaric thermotropic measurements, the first heating scan was performed at heating rate of 0.33 K min^{-1} and after the completion of the first scan, the subsequent second scan was immediately started. In the isothermal barotropic measurements, the pressure was increased by approximately 5 MPa in each step in the vicinity of the phase transition, and the sample solution was allowed to stand for 10 min, in each step.

2.4. Fluorescence measurements under high pressure

The fluorescence measurements under high pressure were carried out referring to our previous work [39]. Fluorescence spectra of Prodan in various phases of lipid bilayers under high pressure were observed by a similar method to the isobaric thermotropic phase transition measurements. As for the measurement, the pressure, at which the heating of high-pressure cell was started, was recorded because the pressure of closed system was slightly elevated by the heating. The accuracy of temperature and pressure in the high-pressure cell was the same as the light-transmittance measurement. The heating rate at a given pressure was 0.50 K min^{-1}. The excitation wavelength was 361 nm, and the emission spectra were observed in the wavelength range from 400 to 600 nm.

The second derivative of the emission spectrum was obtained by an attached software (FL-solutions) and Origin software (OriginLab Corp., Northampton, MA).

3. Results and discussion

3.1. Thermotropic and barotropic phase transitions

The heating DSC thermograms of C17PC bilayer membrane showed three kinds of endothermic transitions in the 1st heating scan after cold storage (curve 1 in Fig. 1A). The three peaks were observed at temperatures of 25.0, 42.9 and 48.6 °C. The phase transition temperatures are summarized in Table 1. The C17PC bilayer underwent three phase transitions with increasing temperature: the subtransition from the subgel (L_c) phase to the lamellar gel (L_{β}') phase, the pretransition from the L_{β}' phase to the ripple gel (P_{β}') phase and finally the main transition from the P_{β}' phase to the liquid crystalline (L_{α}) phase, in turn. However, the subsequent scan (2nd scan), which was reheated immediately after cooling the sample, provided only the pretransition and main-transition peaks (curve 2 in Fig. 1A). The subtransition was observed only in the 1st heating scan after cold storage because the rate of transformation into the L_c phase was extremely slow [40]. This thermal behavior was in good agreement with the previous observations [17,41,42]. In the figure are also depicted the results of asymmetric PC bilayers. The DSC thermograms of the PSPC and SPPC bilayer membranes also showed three endothermic transitions (Fig. 1B and C). The thermal behavior was similar to that of the C17PC bilayer membrane.

The phase transition of lipid bilayers induces abrupt changes in membrane properties. There are several methods for detecting the changes. One of the methods utilizes the change of the turbidity of the phospholipid vesicle suspension, for example, translucent in the liquid crystalline state and less translucent in the gel state, which can be monitored by light absorbance (transmittance) or scattering. Turbidity change mainly results from the change in optical properties of the membrane such as a refractive index, and it is attributable to multiple factors such as changes in vesicle size and in fluctuation of movement between hydrocarbon chains of lipid molecules, etc [43,44]. We adopted the above light-transmittance measurement of vesicle suspension to detect phase transitions under high pressure.

Figure 2 shows the isobaric thermotropic phase transition of the C17PC bilayer membrane by the optical method. The transmittance increased abruptly at a certain temperature corresponding to the phase transition temperature. At ambient pressure, the temperatures of the subtransition, pretransition and main transition were found to be 25.8, 41.8 and 47.7 °C, respectively, which were in good agreement with the temperatures determined by the DSC (curve 1 in Fig. 2A). The 2nd scan showed the pretransition and main transition. The temperatures of these three kinds of transitions increased with an increase in pressure. At pressure of 98.5 MPa, the transmittance showed a different profile from that obtained at ambient pressure. In the 1st scan at constant pressure of 98.5 MPa, we could observe the transition from the L_c phase to the pressure-induced interdigitated gel

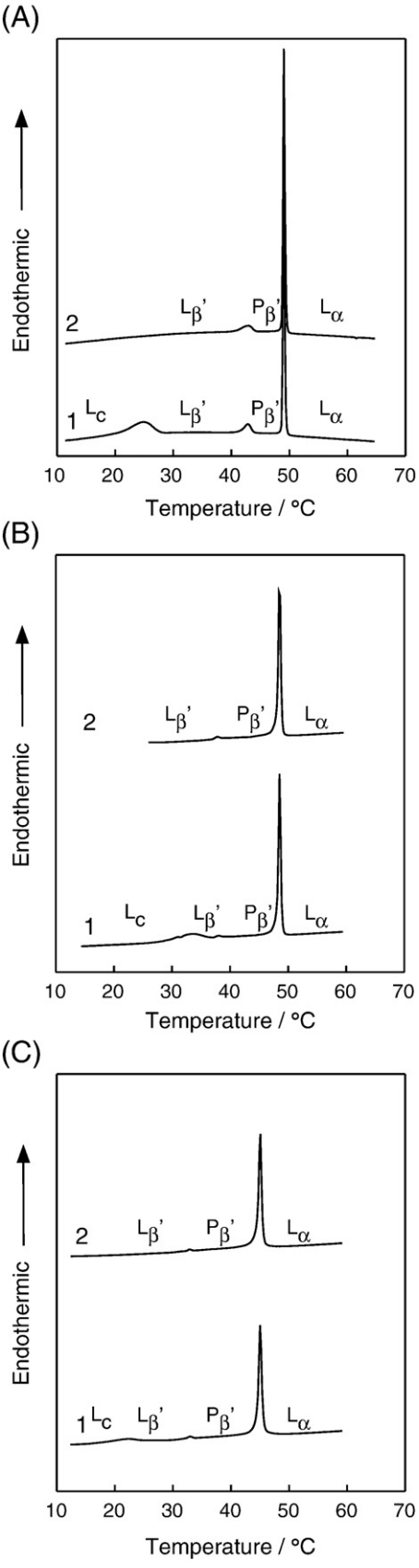

Fig. 1. DSC thermograms for the bilayer membranes of (A) C17PC, (B) PSPC and (C) SPPC; curve 1: 1st heating scan, curve 2: 2nd heating scan.

Table 1
Thermodynamic properties of phase transitions for symmetric and asymmetric PC bilayer membranes obtained from DSC and light-transmittance measurements

Lipid	Transition	Temp. / °C	Temp. / K	dT/dp / K MPa^{-1}	ΔH / kJ mol^{-1}	ΔS / J K^{-1} mol^{-1}	ΔV / cm^3 mol^{-1}
C18PC	P_β'/L_α	55.6[d]	328.8	0.230	45.2[d]	137	31.6
PSPC	P_β'/L_α	48.5±0.06[a]	321.7	0.261	37.1±1.07[a]	115	30.1
C17PC	P_β'/L_α	48.6±0.05[a]	321.8	0.224	41.4±0.76[a]	129	28.8
SPPC	P_β'/L_α	45.0±0.05[a]	318.2	0.271	36.3±1.45[a]	114	30.9
C16PC	P_β'/L_α	42.0[d]	315.2	0.220	36.4[d]	115	25.4
C18PC	L_β'/P_β'	50.9[d]	324.1	0.14	5.0[d]	15.0	2.2
PSPC	L_β'/P_β'	37.5±0.48[a]	310.7	0.08	0.84±0.20[a]	2.7	0.22
C17PC	L_β'/P_β'	42.9±0.19[a]	316.1	0.13	4.6±0.39[a]	15.0	1.9
SPPC	L_β'/P_β'	32.2±0.31[a]	305.4	0.10	0.44±0.11[a]	1.4	0.14
C16PC	L_β'/P_β'	34.3[d]	307.5	0.13	4.6[d]	15.0	1.9
C18PC	L_c/L_β'	28.2[b]	301.4	0.22	28.1[b]	93.2	20.5
PSPC	L_c/L_β'	33.5±0.36[a]	306.7	0.14	18.4[c]	60.0	8.4
C17PC	L_c/L_β'	25.0±1.07[a]	298.2	0.16	27.2[b]	91.2	14.6
SPPC	L_c/L_β'	22.1±0.15[a]	295.3	0.14	23.0[c]	77.9	10.9
C16PC	L_c/L_β'	21.2[b]	294.4	0.18	26.0[b]	88.3	15.9

[a] Each value is denoted as (average±standard deviation) over 6 measurements. [b, c] The thermodynamic quantities of subtransition are based on the ΔH values from the literatures ([b] Lewis et al. [41]. [c] Mattai et al. [25].) because our results were not reproducible. [d] Data from Ichimori et al. [17].

(L_βI) phase, pretransition from the L_βI phase to the P_β' phase and main transition in turn. These phase assignments were performed by reference to previous data of PC analog [13,14,17]. The temperatures of the phase transitions were found to be 40.6, 64.5 and 72.5°C. The L_c/L_βI transition was observed only in the 1st scan, where the transmittance increased abruptly at the transition. Instead of the L_c/L_βI transition, the L_β'/L_βI transition was observed at the repeated heating scan at 41.5°C. In the case of the latter transition, the light transmittance decreased abruptly (curve 2 in Fig. 2B). Similar light-transmittance changes were observed for the DPPC [45], PSPC and SPPC bilayers except for the L_β'/L_βI transition for the SPPC bilayer.

3.2. Phase diagrams of lipid bilayer membranes

The T–p phase diagram of C17PC bilayer is shown in Fig. 3A. The temperatures of the sub-, pre- and main transitions at ambient pressure were 25.0, 42.9 and 48.6°C, respectively, which were in good agreement with the previous results [41]. The slopes of the phase boundaries (dT/dp) at ambient pressure were 0.224 K MPa^{-1} for the main transition, 0.13 K MPa^{-1} for the pretransition and 0.16 K MPa^{-1} for the subtransition, respectively. They were also in good agreement with our previous data [17]. In the high pressure region, a new pressure-induced L_βI phase appeared between the L_β' (or L_c) and P_β' phases. It is noted that at the triple point on the phase diagram, three phases, the L_β', P_β' and L_βI phases, coexist. The value of pressure at the triple point would be defined as a critical interdigitation pressure (CIP). That is, the CIP value can be regarded as the minimum pressure for the interdigitation of lipid bilayer membranes [46]. The slope of phase boundary between the L_β' and L_βI phases varied in the sign from negative to the positive at 125 MPa. This phenomenon suggests that the two phases have different compressibilities [17]. The T–p curves for the L_c/L_βI and L_β'/L_βI transitions intersected each other at about 113 MPa like a DPPC bilayer [45]. Hence, the L_β'/L_βI transition can be recognized as the transformation between metastable phases at pressures above 113 MPa.

As is seen from Fig. 3A, the polymorphism among the gel phases was observed in the C17PC bilayer membrane. Since the choline head group of a lipid molecule is bulky, the acyl chains are tilted away about 30° from the bilayer normal to maintain stable distance between acyl chains in the gel state [47]. Therefore, the chain tilting is responsible for the polymorphism of gel phases such as the L_β', P_β' and L_βI phases. Various amphiphiles like polyols, short-chain alcohols and anesthetics also induce fully interdigitated bilayers of symmetric-chain PCs [48]. The inducers localize at the interface region of the bilayer and substitute for water, producing an increase in the interfacial area per a lipid molecule. It weakens attractive force between head groups, resulting in the positioning of the terminal methyl groups of acyl chains at the bilayer interface region to increase the van der Waals forces between the acyl chains. In comparison with the chemically-induced interdigitation, a mechanism of the pressure-induced interdigitation is still unclear. Although the hydrostatic pressure is propagated equally in all directions, it is known that there is a non-isotropic compression in the case of pressure-induced interdigitation from the P_β' phase to the L_βI phase, namely, a shrinkage of bilayer space and an expansion in the lateral direction [13,14], and also the decrease of total volume [15]. A strong repulsive interaction between polar head groups is presumed to be required transiently for the lateral expansion in bilayers. NMR and neutron diffraction studies indicate that the head groups have a preference for orienting parallel to the plane of the bilayer [49–51]. This suggests that a head group conformation has the positively charged choline group closer to the neighboring negatively charged phosphate group, which brings about an attractive interaction between head groups. Since the compression brings about increasing proximity between lipid molecules, pressure probably induces the conformational change of head group from the parallel to the perpendicular to the bilayer plane. Consequently, we speculate that the bilayer interdigitation may be mainly caused by the transient repulsive interaction between the neighboring polar head groups, which is induced by the transient perpendicular conformation of the head groups under high pressure.

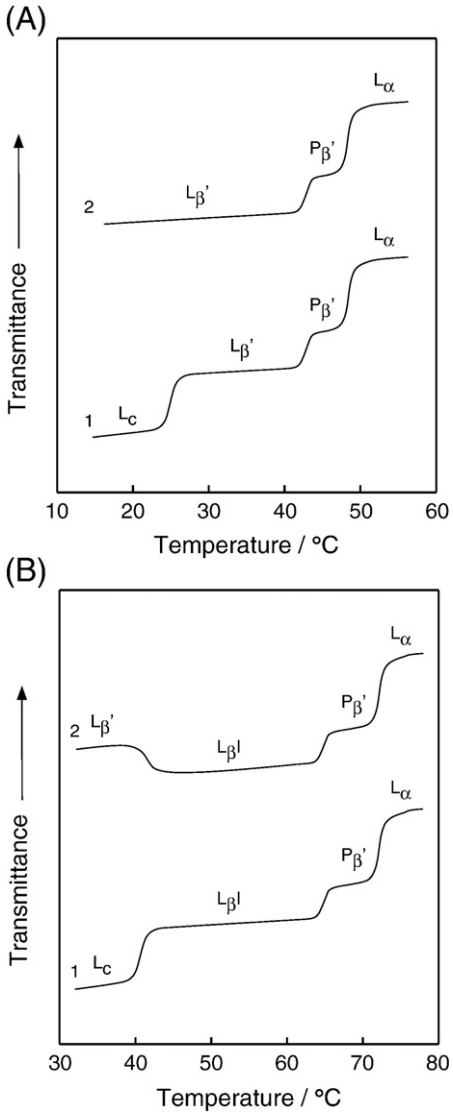

Fig. 2. Phase transitions of C17PC bilayer observed by light-transmittance at (A) 0.1 MPa and (B) 98.5 MPa; curve 1: 1st heating scan, curve 2: 2nd heating scan.

The *T*–*p* phase diagram of the PSPC bilayer membrane is shown in Fig. 3B [46]. The temperatures of the subtransition, pretransition and main transition at ambient pressure were 33.5, 37.5 and 48.5°C, respectively, which are in good agreement with the previous results [25]. The values of d*T*/d*p* for the main, pre- and subtransition were 0.261, 0.08 and 0.14 K MPa^{-1}, respectively. The barotropic phase behavior of the PSPC bilayer is similar to that of the C17PC bilayer. It should be noted that the CIP value of the PSPC bilayer became the smallest among phospholipids in this study.

Fig. 3C shows the *T*–*p* phase diagram of the SPPC bilayer membrane. The temperatures of the subtransition, pretransition and main transition at ambient pressure were 22.1, 32.2 and 45.0°C, respectively. The subtransition temperature was in good agreement with the results of Lin et al. [53] but lower than that of the previous results [21,25]. Our data showed that the difference in the subtransition temperature between the PSPC and SPPC bilayers amounts to 11.4°C. The values of d*T*/d*p* for the main, pre- and subtransition were 0.271, 0.10 and 0.14 K MPa^{-1}, respectively. With respect to the interdigitation of the SPPC bilayer, we observed an unusual profile of the transmittance in the case of transformation from the L_{β}' phase to the $L_{\beta}I$ phase, where the light transmittance under high pressure increased abruptly just before an ordinary decrease. The initial increase in the light transmittance was observed only in the SPPC bilayer and the transition was regarded as stepwise transformation. Therefore, the phase boundary is shown as two lines in Fig. 3C. It is expected that the asymmetry of the two acyl chains of the SPPC bilayer causes the coexistence of the two phases (i.e., L_{β}' and $L_{\beta}I$) during the course from the single L_{β}' to the single $L_{\beta}I$ phase under high pressure, which is shown by a grey-colored zone in the phase diagram.

3.3. Thermodynamic quantities of phase transitions

The thermodynamic quantities, i.e., enthalpy (ΔH), entropy ($\Delta S = \Delta H/T$), and volume (ΔV) changes, of respective phase transitions were obtained from the DSC data and by the application of the d*T*/d*p* value to the Clapeyron equation (d*T*/d*p* = $\Delta V/\Delta S$) [52]. The thermodynamic properties of phase transitions for the symmetric and asymmetric PC bilayers are summarized in Table 1. The thermodynamic data for C16PC and C18PC were taken from previous data [17,41,45], which are also included in Table 1. The values of d*T*/d*p* for the main transition of the asymmetric PC bilayers were larger than those of the symmetric PC bilayers. Regarding the pretransition and subtransition, the values of d*T*/d*p* became slightly smaller in comparison with the symmetric PC bilayers.

The ΔH values of the main transition for the PSPC and SPPC bilayers were 37.1 and 36.3 kJ mol^{-1}, respectively, which are comparable with the values previously reported [25]. They were smaller than that of the C17PC bilayer. The ΔV values of the main transition for the asymmetric PC bilayers were slightly larger than that of the C17PC bilayer. As mentioned before, the acyl chain length at the *sn*-2 position of the glycerol backbone is virtually shortened by 1.5 carbon–carbon lengths relative to that at the *sn*-1 position in the gel state of bilayer membranes for symmetric PCs [36]. In the case of the PSPC and SPPC bilayers, the differences in effective chain length between the *sn*-1 and *sn*-2 chains are 0.5 and 3.5, respectively. Hence, we expected that the PSPC bilayer has the strongest interaction between acyl chains. However, the C17PC bilayer produces the most stable gel state in the acyl chain packing observed from the ΔH values in Table 1. This discrepancy is probably attributable to the chain tilting in the gel phase of these bilayer membranes. In the gel phase with tilting chains, the C17PC bilayer, which has the difference of effective chain length to be 1.5, seems to be more stable than the PSPC bilayer with the difference of 0.5 effective chain length, judging from the fact that the diffraction spacing of the PSPC bilayer is larger than that of the C17PC bilayer [25].

The thermodynamic properties of the pretransition for the PC bilayers are also listed in Table 1. Although the pretransitions of asymmetric PC bilayers have been reported in several papers as

a metastable transitions because of the L_{β}' phase to be unstable [23,25,35], and the pretransition of the PSPC and SPPC bilayers have not been observed in previous results [21], we observed the pretransition as a stable transition in the PSPC and SPPC bilayer membranes. In the present study, the values of ΔH for the asymmetric PC bilayers were extremely smaller than that for the C17PC bilayer. This indicates that for these asymmetric lipid bilayers the partial molar enthalpies of the lipid molecule in the L_{β}' and P_{β}' phases are close to each other.

The subtransition temperature of the SPPC bilayer was 22.1 °C, which was reproducible and in good agreement with the results of Lin et al. [53] but lower than that of the previous results [21,25]. Since the ΔH values were not reproducible due to the dependence of peak area on the period of cold storage, the thermodynamic quantities of subtransition for the bilayers were estimated from the ΔH values in the literatures [25,41]. Interestingly, the temperature difference of the subtransition between the PSPC and SPPC bilayers amounts to 11.4 °C and the subtransition temperature of the C17PC bilayer is within this temperature range. Kodama et al. [42] have demonstrated in the subgel phase of DPPC bilayer by a DSC study that the transformation into the subgel phase took place through dehydration at the adjacent head group of PC molecules. In addition to the dehydration at the head group, the acyl chain packing seems to affect the stability of the L_c phase. The behavior may be clearly related to the acyl chain packing in the bilayer. The acyl chains of three lipid molecules are all tilted in the L_{β}' phase, and the C17PC molecules may have the most stable configuration of the acyl chains in the tilted form. On the other hand, the most cohesive interaction between the acyl chains is seen in the CIP value as mentioned later, where the PSPC bilayer exhibits the strongest interaction as expected from the molecular structure and the bilayer normal form of the acyl chains in the $L_{\beta}I$ phase.

3.4. Comparison of the main-transition temperature and CIP between symmetric and asymmetric PC bilayers

The T–p phase boundaries between the P_{β}' and L_{α} phase for the symmetric and asymmetric PC bilayer membranes are depicted in Fig. 4. With respect to the symmetric PC bilayers, the T–p curves for the main transition were shifted toward higher temperatures as the acyl chains are elongated [17]. Comparing the T–p curves among the PSPC, SPPC and C17PC bilayers, the T–p curve for the PSPC bilayer was slightly shifted toward higher temperatures than that for the C17PC bilayer, while the T–p curve for the SPPC bilayer was conversely lowered. The transition temperatures as a whole are elevated in the order of SPPC, C17PC and PSPC. The order of the temperature elevation is consistent with the order of *sn*-2 acyl chain length. Therefore, it may be concluded that the acyl chain in the *sn*-2 position participates preferentially in the main-transition properties under ambient and high pressures.

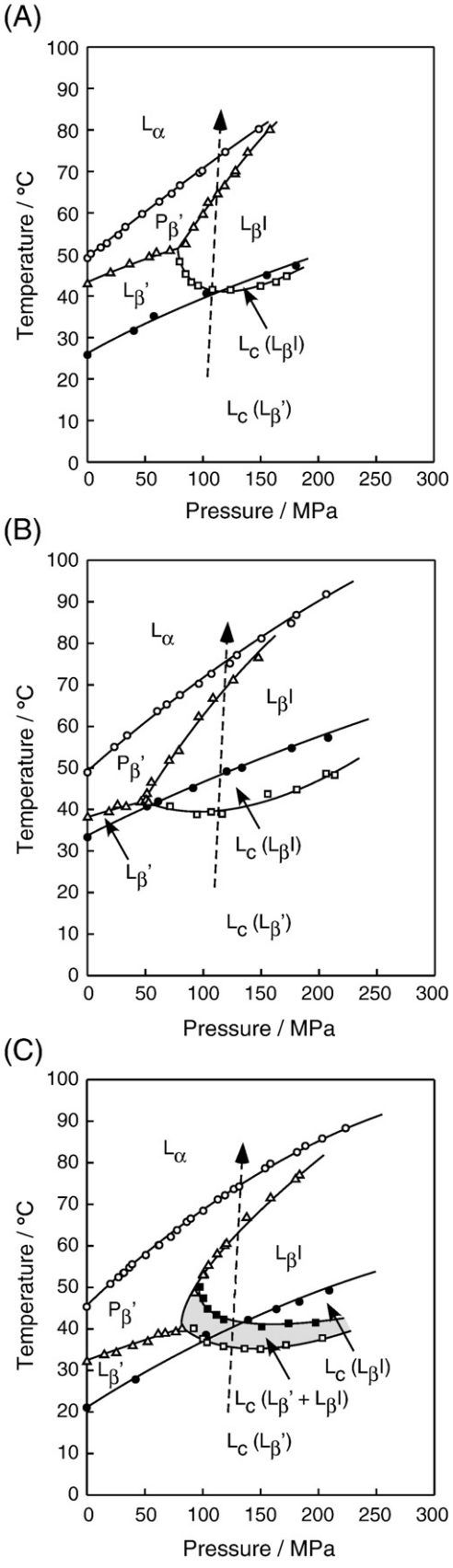

Fig. 3. Temperature–pressure phase diagrams for bilayers of (A) C17PC, (B) PSPC and (C) SPPC. Bilayer phases are assigned as the liquid crystalline (L_{α}), lamellar gel (L_{β}'), ripple gel (P_{β}'), interdigitated gel ($L_{\beta}I$) and subgel (L_c) phases. Bilayer phases in parentheses refer to metastable phase. Broken lines in the phase diagrams represent the heating process under high pressure for measurements of fluorescence spectra shown in Fig. 6.

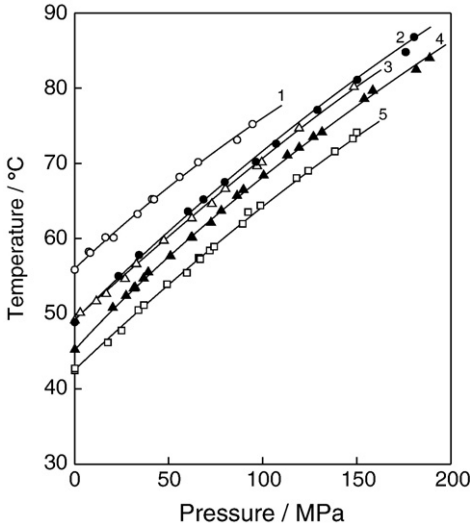

Fig. 4. Temperature–pressure phase boundaries between the ripple gel and liquid crystalline phases for symmetric and asymmetric lipid bilayers; (1) C18PC, (2) PSPC, (3) C17PC, (4) SPPC and (5) C16PC.

The CIP values for the symmetric and asymmetric PC bilayer membranes are plotted as a function of the *sn*-2 acyl chain length in Fig. 5. The previous study for a series of symmetric PC membranes demonstrated that the value of CIP decreases with increasing acyl chain length in a non-linear manner [17]. This fact indicates that the ease of pressure-induced interdigitation of PC bilayers is dependent on the cohesive force between acyl chains of the PC molecule. Although the CIP value for C17PC bilayer amounted to 79.1 MPa, those of the PSPC and SPPC bilayers became 50.6 and 93.0 MPa. The dependence of the *sn*-2 acyl chain length was also found in the interdigitation of asymmetric bilayer membrane. Because the terminal methyl ends of the *sn*-1 and *sn*-2 chains of the PSPC molecule can approach the nearest to each other along the molecular axis in the $L_\beta I$ state, it is probable that the enhanced cohesive interaction between acyl chains reduces the CIP value to lower pressure region.

3.5. Fluorescence spectra of Prodan in lipid bilayers under high pressure

As mentioned before, the $L_\beta'/L_\beta I$ phase transition of the SPPC bilayer observed by the optical method progresses stepwise, whereas the C17PC and PSPC bilayers exhibit ordinary transition profiles. In order to make the interdigitation processes clear, we performed fluorescence measurements on the lipid solutions under high pressure. The fluorescence spectra of Prodan in the bilayer membranes were observed as a function of temperature and pressure. It has been reported that the wavelength of emission maximum (λ_{max}) of Prodan in the symmetric PC bilayers is found to be about 480, 430 and 500 nm for the L_α, L_β' (or P_β') and $L_\beta I$ phase, respectively [39]. The value of λ_{max} depends on the dielectric constant of solvent around the probe molecules at constant temperature and pressure. The Prodan molecules are distributed around the phosphate groups and adjacent glycerol backbones of PCs in the L_α and L_β' (or P_β') phases of the bilayer, respectively. Since the lipid bilayers are transformed into monolayers in the interdigitation, the Prodan molecules are squeezed out from the glycerol backbone region and moves to the hydrophilic region near the bilayer surface.

The fluorescence spectra of Prodan in the C17PC bilayer membranes were observed at 105.6 MPa as a function of temperature; typical spectra at various temperatures are shown in Fig. 6A. In order to make clear the relation between the λ_{max} values and the bilayer phases, the λ_{max} values obtained from Fig. 6 were plotted against temperature under high pressure, as shown in insets. The C17PC bilayer undergoes three phase transitions as the temperature increases: the $L_\beta'/L_\beta I$ phase transition, the pretransition (i.e., the $L_\beta I/P_\beta'$ transition) and finally the main transition. The emission spectrum of Prodan in the C17PC bilayer at about 20°C had a maximum around 451 nm, which corresponds to the Prodan spectrum in the L_β' phase. The values of λ_{max} decreased slightly with increasing temperature and then the drastic shift of λ_{max} from 443 to 493 nm was observed at 42.3 °C. The appearance of the peak at 493 nm is attributable to the bilayer interdigitation. As the temperature increased up to 68.4 °C, the 451 nm peak became significant once again, which corresponds to the Prodan spectrum in the P_β' phase. At 73.0 °C, further increase in temperature brought about the shift of λ_{max} from 451 to 480 nm. The spectrum peak at 480 nm is caused by Prodan in the L_α phase in the bilayer membrane.

Fig. 6B shows the emission spectra of Prodan in the PSPC bilayer at 108.8 MPa. The feature of the spectra resembled that in the C17PC bilayer except for the value of λ_{max} for the $L_\beta I$ phase, where the λ_{max} values of Prodan in the C17PC and PSPC bilayers were 494 and 487 nm, respectively. The slight difference is probably responsible for the chain packing in the interdigitated structure and/or the multiple distribution sites of

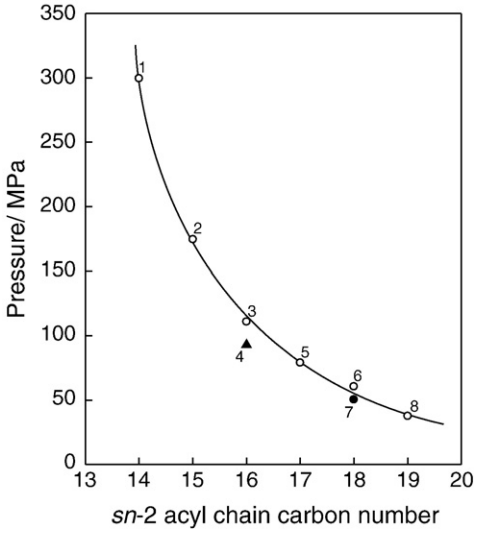

Fig. 5. Critical interdigitation pressure of symmetric and asymmetric lipid bilayers as a function of *sn*-2 acyl chain length; (1) C14PC, (2) C15PC, (3) C16PC, (4) SPPC, (5) C17PC, (6) C18PC, (7) PSPC and (8) C19PC.

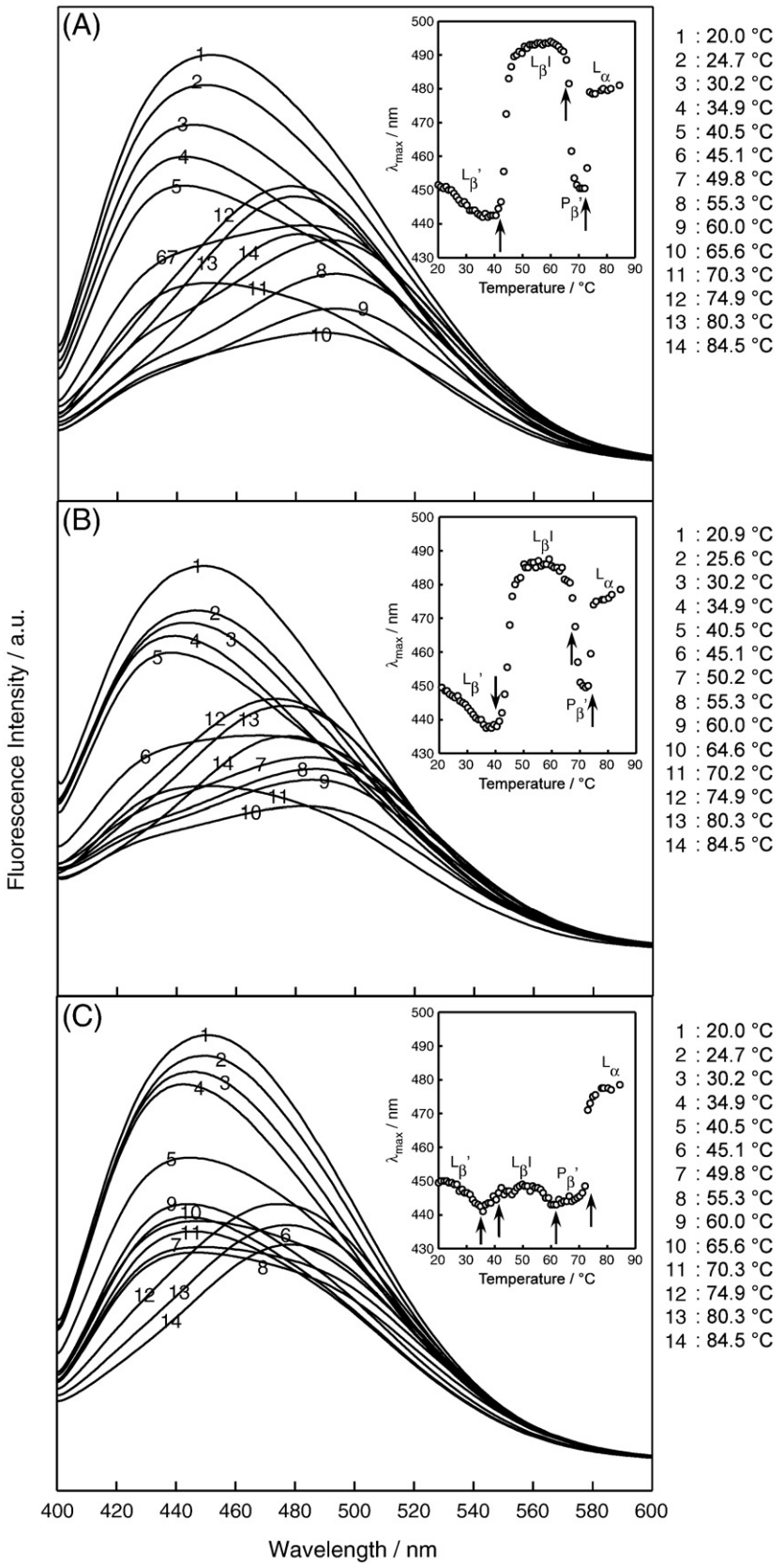

Fig. 6. Fluorescence spectra of Prodan in bilayer of (A) C17PC at 105.6 MPa, (B) PSPC at 108.8 MPa and (C) SPPC at 122.7 MPa as a function of temperature. The insets show the effect of temperature on the maximum emission wavelength of Prodan in the corresponding bilayers. The phase transition temperatures, which were taken from the temperature–pressure phase diagram (Fig. 3), are shown by arrows.

Prodan mentioned later. The fluorescence spectra of Prodan in the SPPC bilayer were also observed as a function of temperature at 122.7 MPa, which are shown in Fig. 6C. Although the SPPC bilayer as well as the C17PC and PSPC bilayers underwent three transitions with increasing temperature, the λ_{max} value for the $L_\beta I$ phase hardly changed. The result suggests that the Prodan molecules in the bilayer membrane are distributed definitely around the glycerol backbone.

The λ_{max} value reflects the distribution of Prodan in the bilayer and responses to the bilayer phase transition [39]. The phase transition temperatures obtained from the *T*–*p* phase diagrams in Fig. 3 are also shown in the insets by arrows. The λ_{max} values in three bilayers decreased gradually with an increase in temperature from 20 °C and subsequently increased abruptly at the temperature of the $L_\beta'/L_\beta I$ transition. In the case of the C17PC and PSPC bilayers, the λ_{max} values increased up to 494 and 487 nm at temperatures just above the transition, respectively. Therefore, we could confirm that the bilayer interdigitation caused the Prodan molecules to move their position to the hydrophilic region. On the other hand, the λ_{max} value for the SPPC bilayer varied stepwise from 441 to 449 nm. The stepwise change and narrow-range variation in λ_{max} correspond to the $L_\beta'/L_\beta I$ transition depicted as a grey-colored zone in the *T*–*p* phase diagram (Fig. 3C), where both of the L_β' and $L_\beta I$ phases probably coexist. The low value of λ_{max} is attributable to the effective chain-length difference of 3.5 carbon–carbon lengths between the *sn*-1 and *sn*-2 chains, that is, the Prodan molecules are still distributed around the glycerol backbone without squeezing out from the bilayer. The asymmetry in the acyl chain lengths may give rise to a "pocket" in the interdigitated bilayer, in which a Prodan molecule can remain. The asymmetry may also be responsible for the coexistence of the L_β' and $L_\beta I$ phases.

3.6. Second derivatives of the emission spectra

In order to analyze a multiplicity of emission spectra in detail, the spectra shown in Fig. 6 were differentiated twice with respect to wavelength at various temperatures. Fig. 7 shows the results of second derivatives of the emission spectra. The second derivative of the emission spectrum serves as a detection tool of minor components in the spectrum: it enables us to detect another component included in the shoulder of the emission spectrum. The second derivative spectrum has been useful in the field of UV/VIS and FT-IR spectroscopy studies [54,55], however, there has been hardly any attempt to apply to the fluorescence spectrum. Since a maximum wavelength in the fluorescence spectrum corresponds to a minimum wavelength in the second derivative curve, we could confirm at least four components in the emission spectra from Fig. 7. Comparing the original emission spectra in Fig. 6 with the second derivatives in Fig. 7, it is obvious that the maximum wavelengths in the original emission spectra are not always consistent with the minimum wavelengths in the second derivative curves. This means that the original emission spectra are composed of multiple components, in other words, the emission spectra of Prodan exhibit the distribution of the Prodan molecules into multiple sites in the bilayer membrane. As is seen from Fig. 7, the second derivative curves exhibited four kinds of minimum wavelengths: 430 ± 1, 433 ± 1, 480 ± 1 and 497 ± 1 nm, respectively, which were common wavelengths to three kinds of lipid bilayers under examination. The two emission components at the wavelengths of 430 and 433 nm were observed at different phases of bilayers, although they were almost similar wavelengths. Therefore, we can conclude that the fluorescence spectra of Prodan in lipid bilayers are composed of at least four emission components, although it is very difficult to distinguish between the L_β' and P_β' phases. The

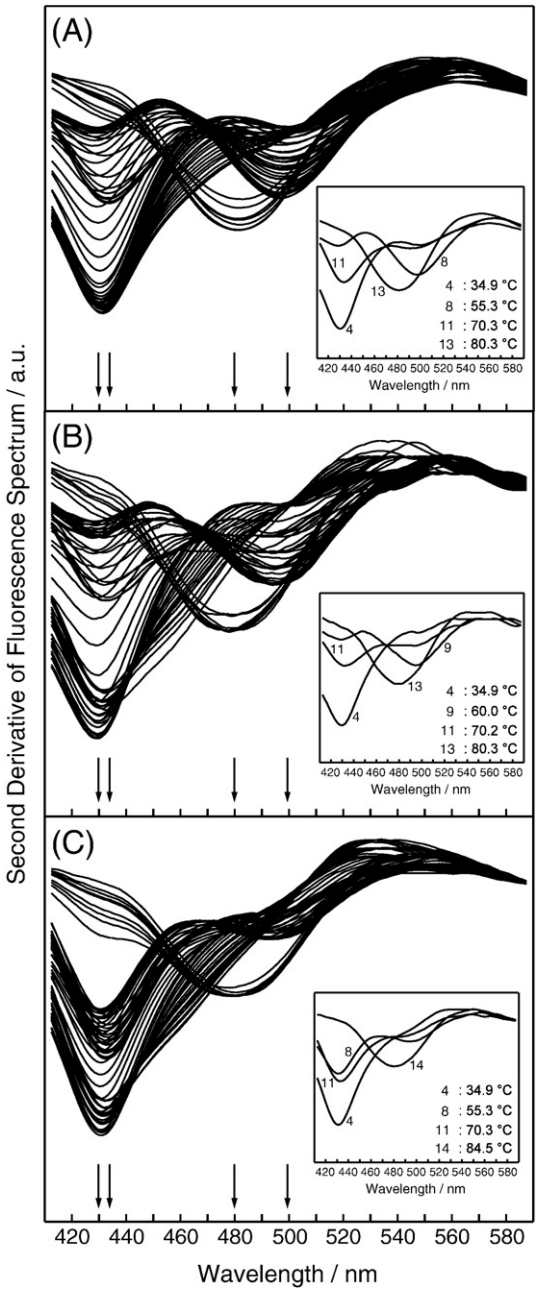

Fig. 7. The second derivatives of fluorescence spectra of Prodan in the bilayers of (A) C17PC, (B) PSPC and (C) SPPC. Second derivative curves, which are depicted by temperature intervals of ca. 1 K, exhibit four kinds of minima at 430, 433, 480 and 497 nm. The insets show the extractions of second derivative curves of each PC bilayer. The spectrum number corresponds to the emission spectrum number in Fig. 6.

wavelengths of emission maxima characteristic of the four phases of the lipid bilayer, i.e., the L_α, P_β', L_β' and $L_\beta I$, primarily correspond to 480, 433, 430 and 497 nm, respectively.

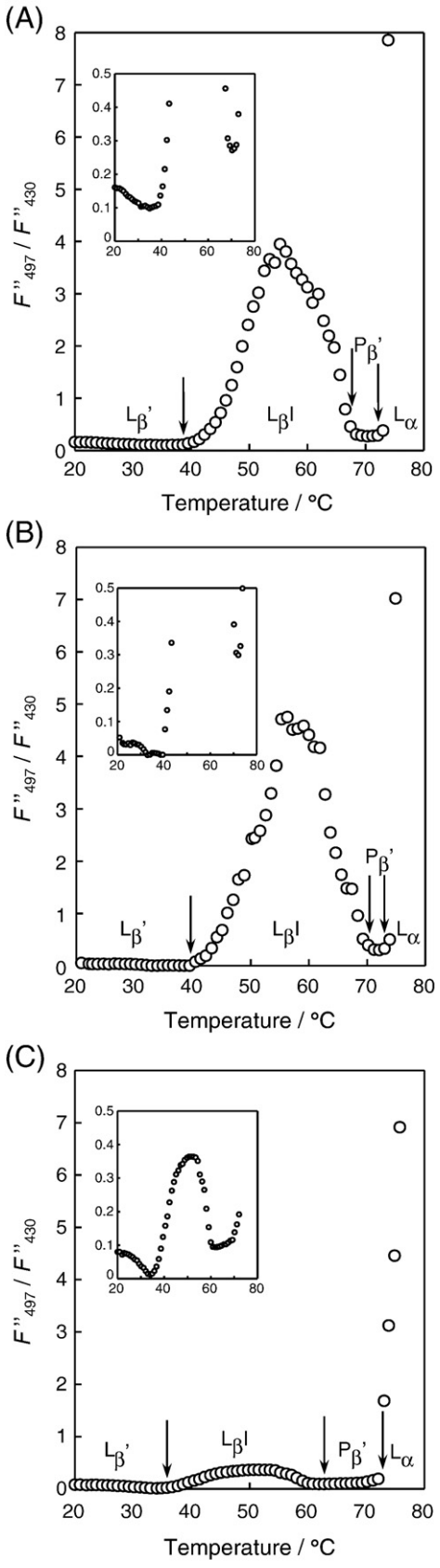

Fig. 8. Ratio of second derivative of fluorescence intensity at 497 nm to that at 430 nm, F''_{497}/F''_{430}, versus temperature plots for Prodan in the bilayer of (A) C17PC at 105.6 MPa, (B) PSPC at 108.8 MPa and (C) SPPC at 122.7 MPa, respectively. The insets show the low values region of F''_{497}/F''_{430} for each PC bilayer.

The Prodan molecules are distributed into two or more locations in the bilayer with varying the quantities in the locations. With respect to the SPPC bilayer, a minimum of second derivative at 497 nm was relatively small, but did not disappear. The result suggests that the Prodan molecules in the $L_\beta I$ phase of the SPPC bilayer are distributed primarily around the glycerol backbone region in a less polar environment rather than the hydrophilic region around lipid head groups. This situation is consistent with the idea that the $L_\beta I$ phase of the SPPC bilayer has a less polar "pocket", in which a Prodan molecule possibly remains, because of the asymmetry of the acyl chain lengths between the *sn*-1 and *sn*-2 chains. Moreover, a ratio of second derivative of fluorescence intensity at 497 nm to that at 430 nm, F''_{497}/F''_{430}, was defined to observe bilayer phase transition. The values of F''_{497}/F''_{430} were plotted against temperature at constant pressure in Fig. 8. The F''_{497}/F''_{430} values in the all bilayers showed a drastic change corresponding to the phase transition and had much higher precision than the previous work which utilized the F_{480}/F_{430} values [39]. Therefore we propose that the values of F''_{497}/F''_{430} are decisive evidence whether interdigitation will occur.

4. Conclusions

The *T*–*p* phase diagrams of the asymmetric PC, PSPC and SPPC, bilayer membranes constructed by DSC and high-pressure light transmittance, and the thermodynamic quantities associated with the phase transitions were compared with those of the symmetric C17PC bilayer. The phase behavior of these PC bilayers was similar to one another except for the transition temperature and pressure. The phase transition temperatures of the SPPC bilayer were lower than those of the PSPC and C17PC bilayers under ambient pressure. The thermodynamic quantities associated with the phase transitions of the asymmetric PC bilayers were lower than those of the C17PC bilayer. The CIP values of the C17PC, PSPC and SPPC bilayer were 79.1, 50.6 and 93.0 MPa, respectively. Contribution of the two acyl chains to the thermodynamic properties associated with phase transitions of the asymmetric PC bilayers was not even under ambient and high pressures. The *sn*-2 acyl chain lengths of asymmetric PCs governed primarily the bilayer properties. The fluorescence spectra of Prodan in the bilayers exhibited the emission maxima characteristic of bilayer phases. Depending on the location of Prodan in the bilayer membranes, the wavelengths of the emission maxima characteristic of the L_α, P_β', L_β' and $L_\beta I$ phases were found to be 480±1, 433±1, 430±1 and 497±1 nm, respectively. The wavelengths were common in all bilayers under examination. The original emission spectra of Prodan in the bilayers were found to be composed of multiple distribution of Prodan. Regarding the second derivatives of fluorescence spectra, the values of F''_{497}/F''_{430} are decisive evidence whether

interdigitation will occur. In the case of the SPPC bilayer, the $L_{\beta}'/L_{\beta}I$ transition under high pressure took place stepwise. Therefore, there existed a two-phase region of coexisting the L_{β}' and $L_{\beta}I$ phases during the course of interdigitation. The emission maximum of Prodan in the SPPC bilayer exhibited the narrow-range red-shift from 441 to 449 nm with the $L_{\beta}'/L_{\beta}I$ phase transition. These results indicate that the $L_{\beta}I$ phase of the SPPC bilayer has a less polar "pocket" formed by a space between uneven terminal methyl ends of the acyl chains, in which a Prodan molecule can remain stably. Consequently, the slightly difference at the terminal methyl ends between the *sn*-1 and *sn*-2 chains significantly affects the phase behavior of the PC bilayers. Our present studies using another asymmetric PCs, myristoylpalmitoyl-PC and palmitoylmyristoyl-PC will clarify this subject in more detail and they will be reported in the near future.

References

[1] K.T. Wann, A.G. Macdonald, Actions and interactions of high pressure and general anesthetics, Prog. Neurobiol. 30 (1988) 271–307.

[2] A.R. Cossins, A.G. Macdonald, The adaptation of biological membranes to temperature and pressure: fish from the deep and cold, J. Bioenerg. Biomembranes 21 (1989) 115–135.

[3] R. Hayashi, C. Balny (Eds.), High Pressure Bioscience and Biotechnology, Elsevier, Amsterdam, 1996.

[4] H. Ludwig (Ed.), Advances in High Pressure Bioscience and Biotechnology, Springer, Heidelberg, 1988.

[5] R. Hayashi (Ed.), Trends in High Pressure Bioscience and Biotechnology, Elsevier, Amsterdam, 2002.

[6] R. Winter (Ed.), Advances in High Pressure Bioscience and Biotechnology, vol. II, Springer, Heidelberg, 2003.

[7] S. Utoh, T. Takemura, Phase transition of lipid multilamellar aqueous suspension under high pressure I. Investigation of phase diagram of dipalmitoyl phosphatidylcholine bimembrane by high pressure-DTA and -dilatometry, Jpn. J. Appl. Phys. 24 (1985) 356–360.

[8] P. Yager, W.L. Peticolas, Statistical mechanical analysis of Raman spectroscopic order parameter changes in pressure-induced lipid bilayer phase transitions, Biophys. J. 31 (1980) 359–370.

[9] P.T.T. Wong, H.H. Mantsch, Effects of hydrostatic pressure on the molecular structure and endothermic phase transitions of phosphatidylcholine bilayers: A Raman scattering study, Biochemistry 24 (1985) 4091–4096.

[10] N.D. Russell, P.J. Collings, High pressure measurements in phospholipid bilayers using adiabatic compression, J. Chem. Phys. 77 (1982) 5766–5770.

[11] P.L.G. Chong, G. Weber, Pressure dependence of 1,6-diphenyl-1,3,5-hexatrien fluorescence in single-component phosphatidylcholine liposomes, Biochemistry 22 (1983) 5544–5550.

[12] J.R. Lakowicz, R.B. Thompson, Differential polarized phase fluorometric studies of phospholipid bilayers under high hydrostatic pressure, Biochim. Biophys. Acta 732 (1983) 359–371.

[13] L.F. Braganza, D.L. Worcester, Hydrostatic pressure induces hydrocarbon interdigitation in single-component phospholipid bilayers, Biochemistry 25 (1986) 2591–2596.

[14] R. Winter, W.C. Pilgrim, A SANS study of high pressure phase transitions in model biomembranes, Ber. Bunsenges. Phys. Chem. 93 (1989) 708–717.

[15] S. Maruyama, H. Matsuki, H. Ichimori, S. Kaneshina, Thermotropic and barotropic phase behavior of dihexadecylphosphatidylcholine bilayer membrane, Chem. Phys. Lipids 82 (1996) 125–132.

[16] D.A. Driscoll, J. Jonas, A. Jonas, High pressure ^{2}H nuclear magnetic resonance study of the gel phases of dipalmitoylphosphatidylcholine, Chem. Phys. Lipids 58 (1991) 97–104.

[17] H. Ichimori, T. Hata, H. Matsuki, S. Kaneshina, Barotropic phase transitions and pressure-induced interdigitation on bilayer membranes of phospholipids with varying acyl chain lengths, Biochim. Biophys. Acta 1414 (1998) 165–174.

[18] K.M.W. Keough, P.J. Davis, Gel to liquid-crystalline phase transitions in water dispersions of saturated mixed-acid phosphatidylcholines, Biochemistry 18 (1979) 1453–1459.

[19] P.J. Davis, B.D. Fleming, K.P. Coolbear, K.M.W. Keough, Gel to liquid crystalline transition temperatures of water dispersions of two pairs of positional isomers of unsaturated mixed-acid phosphatidylcholines, Biochemistry 20 (1981) 3633–3636.

[20] J. Stümpel, A. Niksch, H. Eibl, Calorimetric studies on saturated mixed-chain lecithin–water systems. Nonequivalence of acyl chains in the thermotropic phase transition, Biochemistry 20 (1981) 662–665.

[21] J. Stümpel, H. Eibl, A. Niksch, X-ray analysis and calorimetry on phosphatidylcholine model membranes. The influence of length and position of acyl chains upon structure and phase behaviour, Biochim. Biophys. Acta 727 (1983) 246–254.

[22] K.P. Coolbear, C.B. Berde, K.M.W. Keough, Gel to liquid crystalline phase transitions of aqueous dispersions of polyunsaturated mixed acid phosphatidylcholines, Biochemistry 22 (1983) 1466–1473.

[23] E.N. Serrallach, G.H. de Haas, G.G. Shipley, Structure and thermotropic properties of mixed-chain phosphatidylcholine bilayer membranes, Biochemistry 23 (1984) 713–720.

[24] K.M.W. Keough, B. Giffin, N. Kariel, The influence of unsaturation on the phase transition temperatures of a series of heteroacid phosphatidylcholines containing twenty carbon chains, Biochim. Biophys. Acta 902 (1987) 1–10.

[25] J. Mattai, P.K. Sripada, G.G. Shipley, Mixed-chain phosphatidylcholine bilayers: structure and properties, Biochemistry 26 (1987) 3287–3297.

[26] J.T. Mason, C. Huang, R.L. Biltonen, Calorimetric investigations of saturated mixed-chain phosphatidylcholine bilayer dispersions, Biochemistry 20 (1981) 6086–6092.

[27] S.C. Chen, J.M. Sturtevant, Thermotropic behavior of bilayers formed from mixed-chain phosphatidylcholines, Biochemistry 20 (1981) 713–718.

[28] H. Xu, F.A. Stephenson, C. Huang, Binary mixtures of asymmetric phosphatidylcholines with one acyl chain twice as long as the other, Biochemistry 26 (1987) 5448–5453.

[29] R.N.A.H. Lewis, R.N. McElhaney, F. Osterberg, S.M. Gruner, Enigmatic thermotropic phase behavior of highly asymmetric mixed-chain phosphatidylcholines which form mixed-interdigitated gel phases, Biophys. J. 66 (1994) 207–216.

[30] C. Huang, J.T. Mason, I.W. Levin, Raman spectroscopic study of saturated mixed-chain phosphatidylcholine multilamellar dispersions, Biochemistry 22 (1983) 2775–2780.

[31] P.T.T. Wong, C. Huang, Structural aspects of pressure effects on infrared spectra of mixed-chain phosphatidylcholine assemblies in D_2O, Biochemistry 28 (1989) 1259–1263.

[32] R.N.A.H. Lewis, R.N. McElhaney, Studies of mixed-chain diacyl phosphatidylcholines with highly asymmetric acyl chains: a Fourier transform infrared spectroscopic study of interfacial hydration and hydrocarbon chain packing in the mixed interdigitated gel phase, Biophys. J. 65 (1993) 1866–1877.

[33] R.N.A.H. Lewis, R.N. McElhaney, M.A. Monck, P.R. Cullis, Studies of highly asymmetric mixed-chain diacyl phosphatidylcholines that form mixed-interdigitated gel phases: Fourier transform infrared and ^{2}H NMR spectroscopic studies of hydrocarbon chain conformation and orientational order in the liquid-crystalline state, Biophys. J. 67 (1994) 197–207.

[34] B.A. Lewis, S.K. Das Gupta, G.G. Griffin, Solid-state NMR studies of the molecular dynamics and phase behavior of mixed-chain phosphatidylcholines, Biochemistry 23 (1984) 1988–1993.

[35] C. Huang, J.T. Mason, Structure and properties of mixed-chain phospholipid assemblies, Biochim. Biophys. Acta 864 (1986) 423–470.

[36] T. Bultman, H. Lin, Z. Wang, C. Huang, Thermotropic and mixing behavior of mixed-chain phosphatidylcholines with molecular weights identical with that of l_{α}-dipalmitoylphosphatidylcholine, Biochemistry 30 (1991) 7194–7202.

[37] C. Huang, Mixed-chain phospholipids and interdigitated bilayer systems, Klin. Wochenschr. 68 (1990) 149–165.

[38] A.D. Bangham, J. DeGier, G.D. Grevill, Osmotic properties and water permeability of phospholipids liquid crystals, Chem. Phys. Lipids 1 (1967) 225–246.
[39] M. Kusube, M. Matsuki, S. Kaneshina, Effect of pressure on the Prodan fluorescence in bilayer membranes of phospholipids with varying acyl chain lengths, Colloids Surf., B Biointerfaces 42 (2005) 79–88.
[40] J.F. Nagle, D.A. Wilkinson, Dilatometric studies of the subtransition in dipalmitoylphosphatidylcholine, Biochemistry 21 (1982) 3817–3821.
[41] R.N.A.H. Lewis, N. Mak, R.N. McElhaney, A differential scanning calorimetric study of the thermotropic phase behavior of model membranes composed of phosphatidylcholines containing linear saturated fatty acyl chains, Biochemistry 26 (1987) 6118–6126.
[42] M. Kodama, H. Hashigami, S. Seki, Static and dynamic calorimetric studies on the three kinds of phase transition in the systems of L- and DL-dipalmitoylphosphatidylcholine/water, Biochim. Biophys. Acta 814 (1985) 300–306.
[43] P.N. Yi, R.C. MacDonald, Temperature dependence of optical properties of aqueous dispersions of phosphatidylcholine, Chem. Phys. Lipids 11 (1973) 114–134.
[44] A.F. Behof, R.A. Koza, L.E. Lach, P.N. Yi, Phase transition in phosphatidylcholine dispersion observed with an interferential refractometer, Biophys. J. 22 (1978) 37–48.
[45] M. Kusube, M. Matsuki, S. Kaneshina, Thermotropic and barotropic phase transitions of *N*-methylated dipalmitoylphosphatidylethanolamine bilayers, Biochim. Biophys. Acta 1668 (2005) 25–32.
[46] H. Matsuki, M. Goto, M. Kusube, N. Tamai, S. Kaneshina, Barotropic phase transitions of 1-palmitoyl-2-stearoylphosphatidylcholine bilayer membrane, Chem. Lett. 24 (2005) 270–271.
[47] T.J. McIntosh, Differences in hydrocarbon chain tilt between hydrated phosphatidylethanolamine and phosphatidylcholine bilayers. A molecular packing model, Biophys. J. 29 (1980) 237–245.
[48] J.L. Slater, C. Huang, Interdigitated bilayer membranes, Prog. Lipid Res. 27 (1988) 325–359.
[49] P.L. Yeagle, W.C. Hutton, C. Huang, R.B. Martin, Structure in the polar head region of phospholipid bilayers: a ^{31}P [^{1}H] nuclear overhauser effect study, Biochemistry 15 (1976) 2121–2124.
[50] R.G. Griffin, L. Powers, P.S. Pershan, Head-group conformation in phospholipids: a phosphorus-31 nuclear magnetic resonance study of oriented monodomain dipalmitoylphosphatidylcholine bilayers, Biochemistry 17 (1978) 2718–2722.
[51] G. Büldt, H.U. Gally, J. Seelig, G. Zaccai, Neutron diffraction studies on phosphatidylcholine model membranes. I. head group conformation, J. Mol. Biol. 134 (1979) 673–691.
[52] H. Ichimori, T. Hata, T. Yoshioka, H. Matsuki, S. Kaneshina, Thermotropic and barotropic phase transition on bilayer membranes of phospholipids with varying acyl chain-length, Chem. Phys. Lipids 89 (1997) 97–105.
[53] H. Lin, Z. Wang, C. Huang, Differential scanning calorimetry study of mixed-chain phosphatidylcholines with a common molecular weight identical with diheptadecanoylphosphatidylcholine, Biochemistry 29 (1990) 7063–7072.
[54] T. Ichikawa, H. Terada, Second derivative spectrophotometry as an effective tool for examining phenylalanine residues in proteins, Biochim. Biophys. Acta 494 (1977) 267–270.
[55] W. Dzwolak, M. Kato, A. Shimizu, Y. Taniguchi, FTIR study on heat-induced and pressure-assisted cold-induced changes in structure of bovine α-lactalbumin: stabilizing role of calcium ion, Biopolymers 62 (2000) 29–39.